Rapid microtubule-independent dynamics of Cdc20 at kinetochores and centrosomes in mammalian cells

Marko J. Kallio,[1] Victoria A. Beardmore,[1] Jasminder Weinstein,[2] and Gary J. Gorbsky[1]

[1]University of Oklahoma Health Sciences Center, Oklahoma City, OK 73104
[2]Amgen Inc., Thousand Oaks, CA 91320

Cdc20 is a substrate adaptor and activator of the anaphase-promoting complex/cyclosome (APC/C), the E3 ubiquitin ligase whose activity is required for anaphase onset and exit from mitosis. A green fluorescent protein derivative, Cdc20–GFP, bound to centrosomes throughout the cell cycle and to kinetochores from late prophase to late telophase. We mapped distinct domains of Cdc20 that are required for association with kinetochores and centrosomes. FRAP measurements revealed extremely rapid dynamics at the kinetochores ($t_{1/2}$ = 5.1 s) and spindle poles ($t_{1/2}$ = 4.7 s). This rapid turnover is independent of microtubules. Rapid transit of Cdc20 through kinetochores may ensure that spindle checkpoint signaling at unattached/relaxed kinetochores can continuously inhibit APC/C^{Cdc20} targeting of anaphase inhibitors (securins) throughout the cell until all the chromosomes are properly attached to the mitotic spindle.

Introduction

Trafficking of cell cycle regulatory proteins within the mitotic spindle may be essential in controlling the accurate timing of cell division (Gorbsky et al., 1999; Gorbsky, 2001). Cdc20 is an activator and substrate-specific adaptor protein for the mitotic ubiquitin ligase called the anaphase-promoting complex/cyclosome (APC/C)* (for review see Vodermaier, 2001). Cdc20 targets the anaphase inhibitors Pds1/securin by facilitating a physical link between the APC/C and the target molecule. Mad2, Mad3/BubR1, and Bub3, members of the Mad and Bub spindle checkpoint protein families, restrain the APC/C from targeting Pds1/securin proteins before the alignment of the chromosomes at the metaphase plate. These proteins appear to inhibit APC/C by binding to Cdc20 (Fang et al., 1998; Kallio et al., 1998; Chan et al., 1999). The various checkpoint proteins may function independently or cooperatively to block the targeting of substrates by APC/C^{Cdc20} (Sudakin et al., 2001; Tang et al., 2001; Fang, 2002).

Many of the mitotic checkpoint proteins and regulators of the APC/C, including Cdc20, Bub1, Mad3/BubR1, Bub3, Mad1, and Mad2, associate with kinetochores and centrosomes, often at specific times in the cell cycle (Chen et al., 1996; Li et al., 1997; Kallio et al., 1998; Taylor et al., 1998). These data have led to increasingly detailed models that unattached kinetochores foster the assembly of inhibitory proteins onto the APC/C and/or Cdc20, thus restraining APC/C^{Cdc20} from targeting securins (Kallio et al., 1998; Chen et al., 1998; Sudakin et al., 2001, Sironi et al., 2002). Howell et al. (2000) used FRAP measurements to show that Mad2 is a transient component of the spindle poles and kinetochores with a turnover halftime of 24–28 s. Furthermore, the authors observed that Mad2 is transported between the kinetochores and spindle poles, and this transfer depends on intact spindle microtubules. Here, we quantitatively examine the subcellular localization and dynamics of full length and mutant Cdc20 in living cells using high-resolution fluorescence microscopy and FRAP.

Results and discussion

Cdc20–GFP binds to Mad2, BubR1, and APC/C and does not inhibit mitotic progression in living cells

To determine whether Cdc20–GFP recapitulates the normal intermolecular association of endogenous Cdc20 we used anti-GFP antibody to immunoprecipitate Cdc20–GFP from mitotic (8–12 h in taxol or nocodazole) extracts of transiently transfected HeLa cells. When the immunoprecipitate was
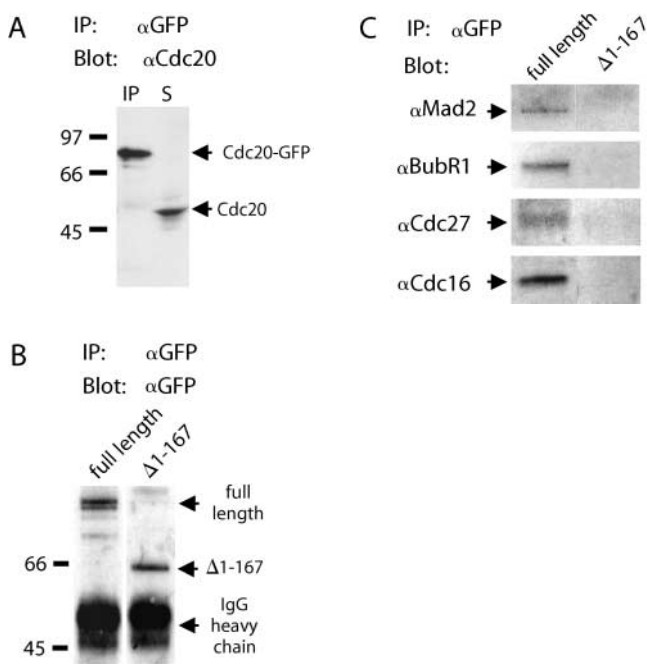
Figure 1. **Cdc20–GFP complexes with the APC/C proteins Cdc27 and Cdc16 and with spindle checkpoint proteins Mad2 and BubR1 in mitotic HeLa cell extracts.** (A) Extracts prepared from cells expressing full-length Cdc20–GFP and blotted with goat anti-Cdc20 antibody show a single band in the immunoprecipitate lane (IP) at ~82 kD (arrowhead). Endogenous Cdc20 (asterisk) remains in the supernatant (S). (B) Anti-GFP immunoprecipitates from cells expressing full-length Cdc20–GFP or truncated Cdc20–GFP$_{\Delta1-167}$ show comparable levels of expression. (C) Anti-GFP immunoprecipitates from cell extracts expressing full-length Cdc20–GFP contain Mad2, BubR1, Cdc27, and Cdc16. Immunoprecipitates from cell extracts expressing Cdc20–GFP$_{\Delta1-167}$ lack association with these proteins.

probed with an anti-Cdc20 antibody, a single ~82-kD protein band was found (Fig. 1 A), which corresponds to the expected size of the Cdc20–GFP chimera. All endogenous Cdc20 remained in the supernatant, suggesting that only one copy of Cdc20 is present in checkpoint complexes in vivo. We compared anti-GFP immunoprecipitates of extracts prepared from mitotic cells expressing full-length Cdc20 or an NH$_2$-terminal deletion, Cdc20–GFP$_{\Delta1-167}$, that lacks the Mad2-binding domain (Fig. 1 B). Mad2, BubR1, and the core APC/C proteins, Cdc27 and Cdc16, were detected in immunoprecipitates of full-length Cdc20 but not Cdc20–GFP$_{\Delta1-167}$, confirming that the NH$_2$-terminal region of Cdc20 is required for association with Mad2, BubR1, and the APC/C (Fig. 1 C).

Cdc20–GFP associates with centrosomes throughout the cell cycle and with kinetochores in M phase

The localization and dynamics of Cdc20–GFP were analyzed in living LLC-PK cells transiently transfected with a plasmid encoding Cdc20–GFP. Chromosome movements in prometaphase and anaphase, the timing of the metaphase–anaphase transition, and exit from M phase all occurred normally in these cells, suggesting that expression of Cdc20–GFP did not impair progression through mitosis.

Furthermore, Cdc20–GFP cells treated with nocodazole arrested at M phase for several hours (Fig. S1, available at http://www.jcb.org/cgi/content/full/jcb.200201135/DC1).

In interphase cells, Cdc20–GFP was concentrated in the nucleus but excluded from the nucleolus. Substantial amounts were also cytoplasmic with a strong concentration at the centrosome. Association with the centrosome persisted throughout the entire cell cycle (Fig. 2 A). In early mitosis, Cdc20–GFP accumulated at the kinetochores, at the spindle poles, and along kinetochore microtubules (Fig. 2 A). During prometaphase, kinetochores near the spindle poles were more intense compared with kinetochores near the spindle equator (Fig. 2 A). We did not detect differences in the fluorescence intensities of the leading and trailing kinetochores of prometaphase chromosomes during their migration to the metaphase plate (Fig. S2 and Video 1, available at http://www.jcb.org/cgi/content/full/jcb.200201135/DC1). The Cdc20–GFP colocalized with the Crest kinetochore marker in M phase (Fig. 2 B). When late prometaphase or metaphase cells were treated with the spindle-disrupting agent nocodazole, the intensity of all kinetochore signals increased to the maximal level (Fig. 2 C), suggesting that the amount of Cdc20 associated with kinetochores is partially and inversely dependent on microtubule occupancy. In nondrug-treated cells, the peak intensity of fluorescence at kinetochores was reached 1–3 min after nuclear envelope breakdown (NEB; Fig. 2 D), and Cdc20–GFP remained associated with the kinetochores from late prophase to late telophase (Fig. 2, B and D). After onset of anaphase, the kinetochore Cdc20–GFP signal diminished rapidly and became indistinguishable from the background as the cells exited mitosis (Fig. 2, B and D). The intensity of diffuse cytoplasmic Cdc20–GFP also decreased substantially during anaphase and telophase, consistent with the findings that Cdc20 is proteolyzed as cells progress to G1 (Weinstein, 1997). In contrast to the loss of Cdc20 at kinetochores and in the cytoplasm, the intensity of Cdc20–GFP at the spindle poles remained high throughout mitosis and after the cells had exited mitosis (Fig. 2 B).

We quantified the distribution of endogenous Cdc20 in mitotic cells by measuring fluorescence intensities after immunolabeling endogenous Cdc20 in fixed cells ($n = 5$) and comparing these data with measurements of Cdc20–GFP fluorescence in living, transfected cells ($n = 5$). In good agreement, both approaches revealed that during mitosis, >80% of Cdc20 was diffusely distributed in the cytoplasm with the remainder concentrated on the poles, spindle fibers, and kinetochores (Fig. 2 E).

Distinct domains of Cdc20 mediate localization to kinetochores and centrosomes

In cell extracts, the Cdc20 protein is found in a variety of complexes with spindle checkpoint proteins and with the APC/C. It is unclear if these different populations localize to different subcellular sites. The Cdc20 protein consists of an NH$_2$-terminal region (amino acids 1–167) that contains putative destruction boxes and domains involved in binding to the APC/C and to the checkpoint protein Mad2 (Zhang and Lees, 2001). After that are seven WD-40 repeats that
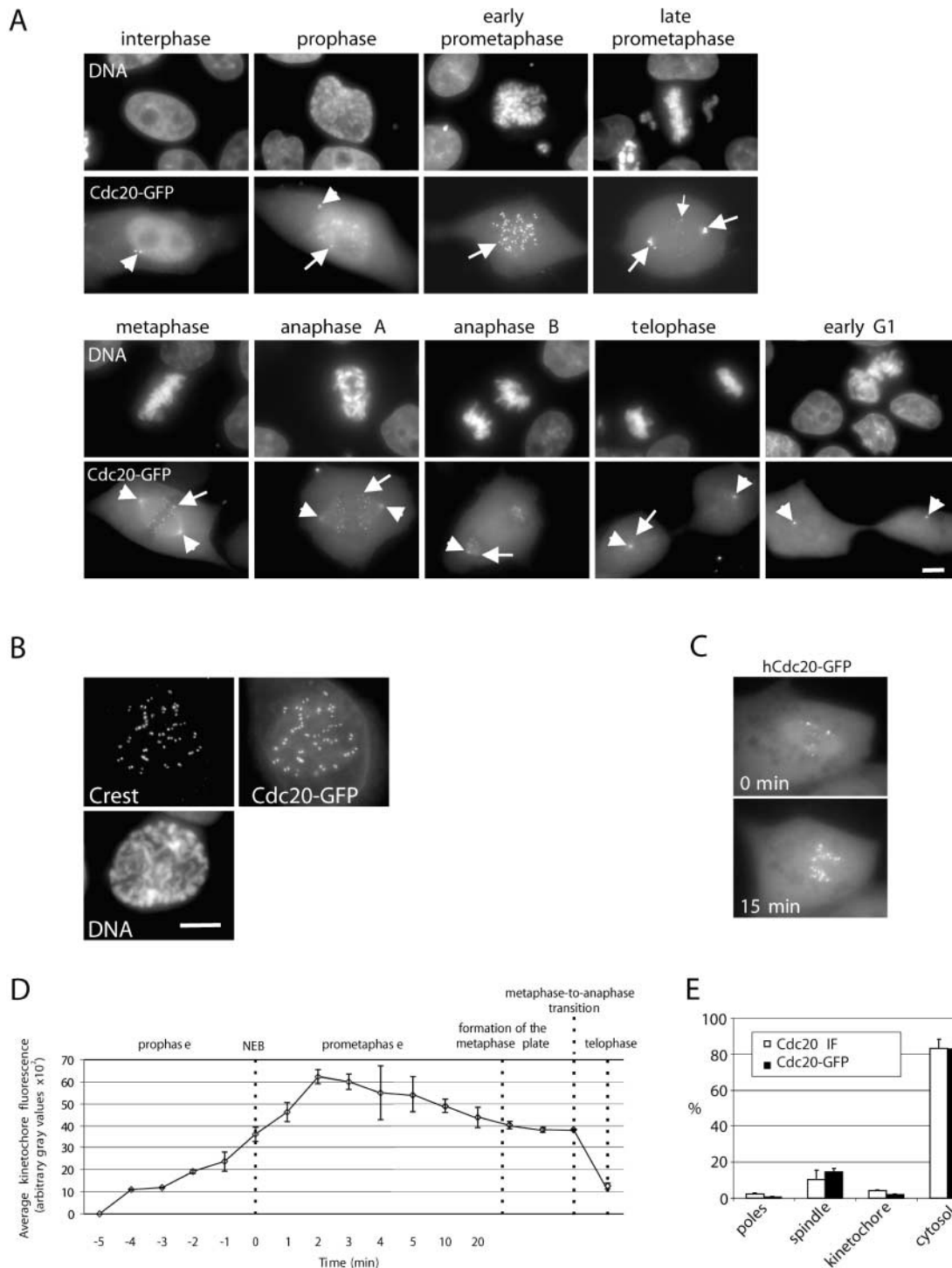
Figure 2.   **Cell cycle–dependent changes in localization of Cdc20–GFP.** (A) At interphase, Cdc20–GFP was concentrated within the nucleoplasm outside the nucleolus. Substantial amounts of Cdc20–GFP were also diffusely distributed in the cytoplasm with a concentration at the centrosomes that persisted throughout the cell cycle (arrowheads). At mitosis, Cdc20–GFP accumulated at the kinetochores from late prophase to late telophase (arrows) and was also present at the spindle poles (arrowheads) and along kinetochore fiber microtubules. More Cdc20–GFP was associated with kinetochores of chromosomes near the poles (late prometaphase cell, large arrows) than with chromosomes at the metaphase plate (small arrow). In anaphase and telophase cells, the kinetochore-bound Cdc20–GFP was diminished (arrows) while remaining at the spindle poles (arrowheads). (B) Cdc20–GFP colocalized with autoimmune antikinetochore immunolabel in M phase. (C) Treatment with nocodazole enhances the intensity of Cdc20–GFP to the maximum level at every kinetochore. A living, transfected LLC-PK cell was treated with nocodazole. Images were taken before (0 min) and 15 min after addition of the drug. (D) Quantization of fluorescence intensities at kinetochores through mitosis. Initial kinetochore accumulation started before NEB, and maximum intensity of kinetochore-bound fluorescence occurred 2–3 min after NEB. After onset of anaphase, Cdc20–GFP was lost rapidly from the kinetochores and was near background levels by telophase. (E) Distribution of endogenous Cdc20 and Cdc20–GFP pools in metaphase cells. The relative amount of Cdc20 at the spindle poles, kinetochores, spindle apparatus, and in the cytosol was determined in fixed cells immunolabeled with anti-Cdc20 antibodies and in live cells expressing Cdc20–GFP. Bars, 5 μm.
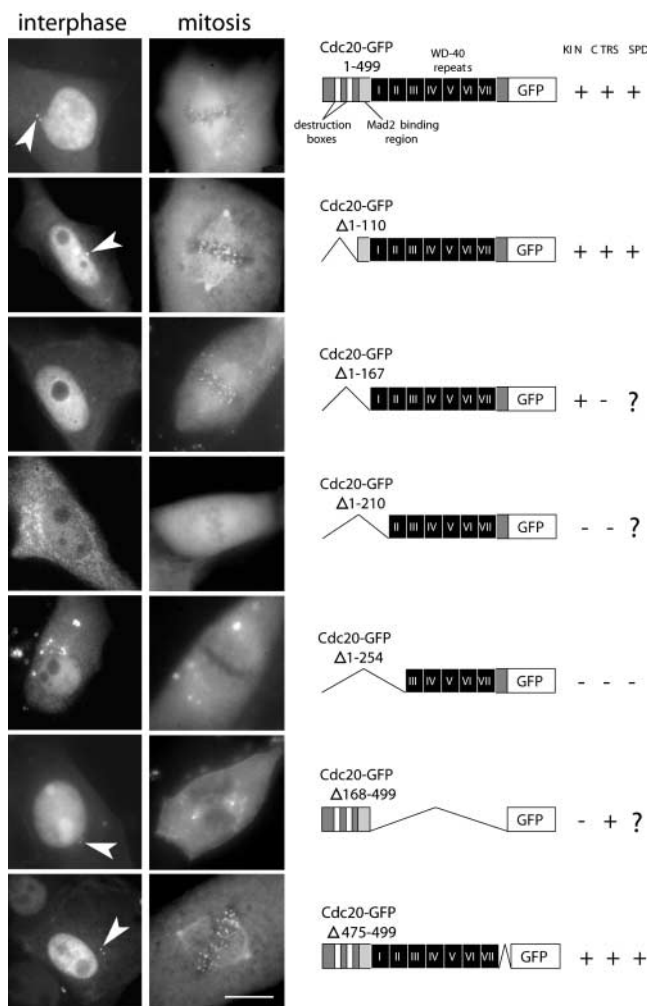
Figure 3. Different domains mediate association of Cdc20–GFP to different subcellular locations. The region from 110–167 amino acids appears to contain a domain required for accumulation of the fusion protein at interphase and mitotic centrosomes (arrowheads). The complete WD-40 array appears to be required for localization of the fusion protein to kinetochores. CTRS, centrosomes; KIN, kinetochores; SPD, spindle fibers. Bar, 5 μm.

form a β-propeller structure and may be involved in binding to substrates (Hilioti et al., 2001). We found that the NH$_2$-terminal region containing the Mad2-binding domain is required for localization to centrosomes, whereas the WD-40 repeats are necessary for localization to kinetochores and spindle microtubules (Fig. 3). A short deletion of the NH$_2$ terminus (Δ1–110), which retains the Mad2-binding domain, had no obvious effect on localization in interphase and mitosis. In contrast, a longer NH$_2$-terminal deletion (Δ1–167), which removes the Mad2/APC/C-binding domain eliminated binding to interphase and mitotic centrosomes but preserved localization at mitotic kinetochores (Fig. 3). A construct containing only the first 167 amino acids and lacking all WD-40 repeats (Δ168–499) showed centrosome and spindle pole localization but did not bind kinetochores. Deletion of the entire NH$_2$ terminus, including the first WD-40 repeat, eliminated binding to both kinetochores and centrosomes. These findings indicate that associ-

ation of Cdc20 with kinetochores requires the WD-40 repeats. In contrast, Cdc20 localization to centrosomes requires the Mad2/APC/C-interacting domain and thus may be due to interaction with Mad2 or APC/C concentrated there.

Cdc20–GFP turns over rapidly at kinetochores and centrosomes

Unattached kinetochores may provide a platform for the assembly/activation of spindle checkpoint complexes with the APC/C (Chen et al., 1998; Kallio et al., 1998). Howell et al. (2000) used FRAP to demonstrate that fluorescent derivatives of the checkpoint protein Mad2 transiently associate with kinetochores and spindle poles, exhibiting half-times of ∼26 s and ∼23 s, respectively. We used FRAP to analyze the turnover of Cdc20–GFP at the kinetochores and centrosomes of LLC-PK cells.

First we determined that photobleaching of Cdc20–GFP did not induce defects in chromosome movements or cell cycle progression (unpublished data). The recovery of Cdc20–GFP was very rapid at kinetochores and centrosomes with average half-times of 5.1 ± 3.6 s ($n = 11$) and 4.7 ± 3.6 s ($n = 7$), respectively (Fig. 4 A; Table I; Video 2, available at http://www.jcb.org/cgi/content/full/jcb.200201135/DC1). At kinetochores, recovery rates were similar from prometaphase to metaphase. In anaphase cells ($n = 5$), recovery of kinetochores was somewhat faster ($t_{1/2} = 3.3 ± 1.4$ s). Recovery of Cdc20–GFP at interphase centrosomes was also rapid ($t_{1/2} = 6.9 ± 3.3$ s, $n = 7$; Fig. 4 B; Table I; Video 3, available at http://www.jcb.org/cgi/content/full/jcb.200201135/DC1). The average turnover of Cdc20–GFP in the cytoplasm was significantly faster (P < 0.05, 2.7 ± 1.0 s, $n = 8$; Table I) than that of kinetochores and centrosomes. The total extent of recovery was from 80 to 94% at centrosomes and kinetochores (Table I), suggesting that most Cdc20 associated with these structures exchanges rapidly. The treatment of cells with microtubule drugs, nocodazole or taxol, did not significantly affect recovery at kinetochores or centrosomes (Table I; Fig. 4 C; Video 4, available at http://www.jcb.org/cgi/content/full/jcb.200201135/DC1).

Cdc20–GFP lacking the Mad2-binding domain (Δ1–167) localizes at kinetochores but not centrosomes. FRAP analysis of Cdc20–GFP$_{\Delta1-167}$ at kinetochores showed rapid half-times for recovery (5.2 ± 3.6 s) and high maximal recovery (82 ± 16%), numbers not different from those of full-length Cdc20–GFP (Fig. 4 D; Table I). Again, treatment of Cdc20–GFP$_{\Delta1-167}$-expressing cells with nocodazole did not alter recovery half-time or extent (Fig. 4 E; Table I).

The role of Cdc20 protein dynamics in the spindle checkpoint

Like Mad2, Cdc20 associates with mitotic kinetochores and spindle poles transiently. However, Cdc20 exchange occurs approximately four times as fast as the published rates for Mad2. Kinetochore-associated Cdc20 exchanges rapidly with the cytoplasmic pool, independent of spindle microtubules. Thus, the trafficking of Cdc20 is distinct from that of Mad2 and may relate to how the checkpoint signal is broadcast throughout the cell from unattached kinetochores.

Table I. **Photobleaching recovery of Cdc20–GFP at kinetochores and centrosomes in living LLC-PK cells**

Target	Treatment	Half-time[a]	Recovery of fluorescence	n
		s	%	
Cdc20–GFP				
Cytoplasm[b]	–	2.7 ± 1.0[c]	76 ± 6	8
Interphase centrosome	–	6.9 ± 3.3	86 ± 14	7
Interphase centrosome	nocodazole	6.3 ± 3.9	94 ± 7	7
Interphase centrosome	taxol	4.0 ± 2.5	77 ± 17	7
Spindle pole	–	4.7 ± 3.6	87 ± 13	7
Kinetochore	–	5.1 ± 3.6	80 ± 9	11
Kinetochore	nocodazole	6.4 ± 4.1	80 ± 12	11
Kinetochore	taxol	4.1 ± 3.4	84 ± 14	11
Cdc20–GFP$_{\Delta1-167}$				
Kinetochore	–	5.2 ± 3.6	82 ± 16	10
Kinetochore	nocodazole	6.2 ± 4.3	79 ± 13	10
α-Tubulin–GFP[d]	–	47.5 ± 13.8	89 ± 12	10

[a]Mean ± SD.
[b]Data from four interphase and four mitotic cells was pooled.
[c]Significantly ($P < 0.05$) different from other values except taxol-treated cells.
[d]The dynamics of interphase microtubule network of LLC-PK tubulin–GFP cell line was measured.

Some years ago, we proposed a model whereby transient association of Cdc20 with unattached kinetochores served to maintain inhibition of the APC/C toward targets whose ubiquitylation and degradation are required for anaphase onset (Kallio et al., 1998). The work reported here and studies from other laboratories support this basic conceptual framework. We now propose refinements to this model (Fig. 5). Kinetochores lacking microtubule attach-
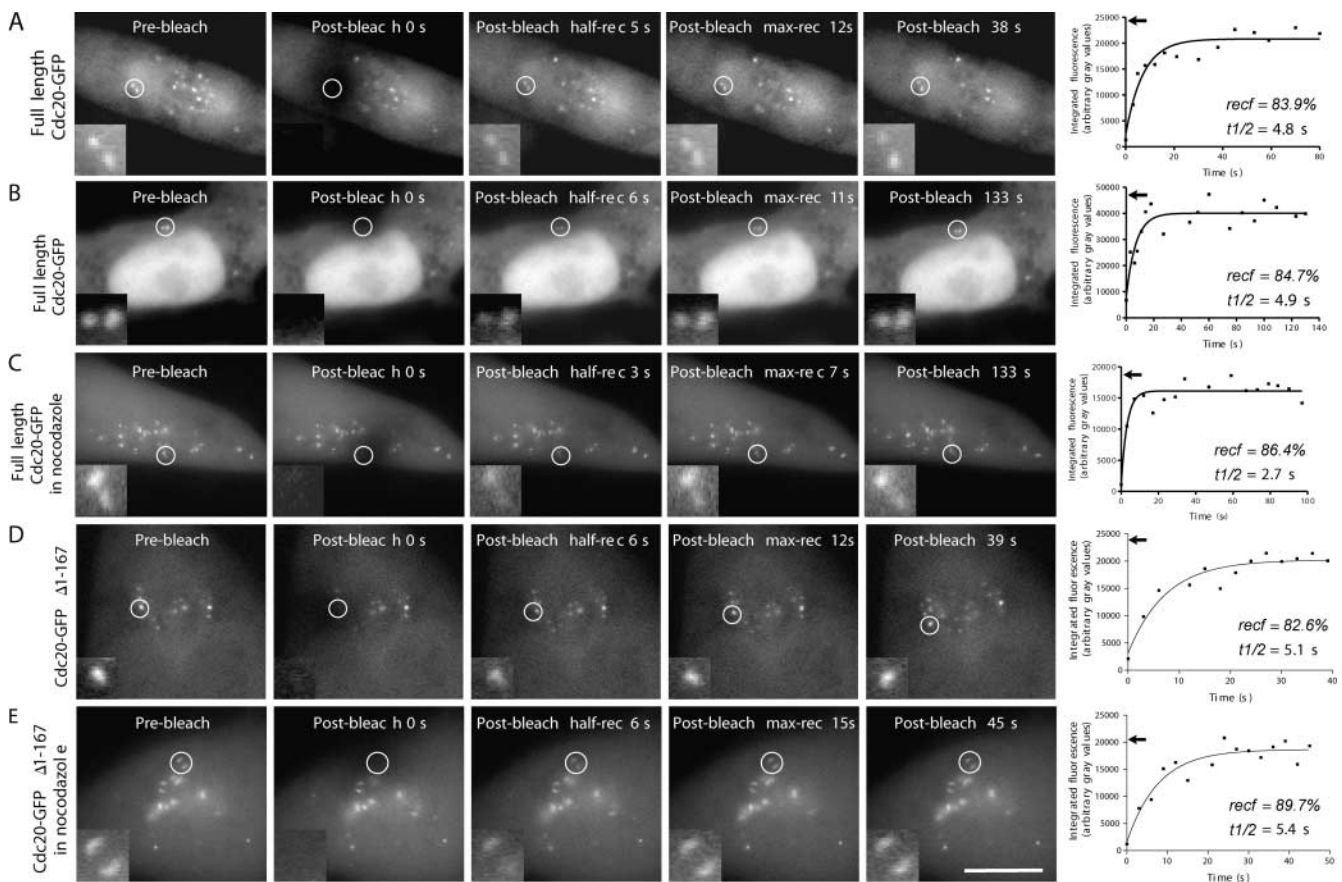

Figure 4. **FRAP analysis of Cdc20–GFP and Cdc20–GFP$_{\Delta1-167}$ turnover in mitotic LLC-PK cells.** (A–E) The kinetochores and centrosomes (white circles) were targeted for laser photobleaching and followed by fluorescence time-lapse microscopy. Prebleach, postbleach, half recovery, and maximal recovery images are shown. The insets show higher magnification views of the target area. The recovery of kinetochore- and centrosome-bound Cdc20–GFP was rapid and independent of microtubules (C and E, nocodazole treatment). At the end of each row are the corresponding graphs of Cdc20–GFP recovery. Arrows indicate prebleached fluorescence of the target area. Percentage of fluorescence recovery (recf) and half-time of recovery ($t_{1/2}$) are shown for each graph. Bar, 10 μm. Supplemental Videos 2–4, corresponding to the still images of panels A, B, and C, respectively, are available at http://www.jcb.org/cgi/content/full/jcb.200201135/DC1.
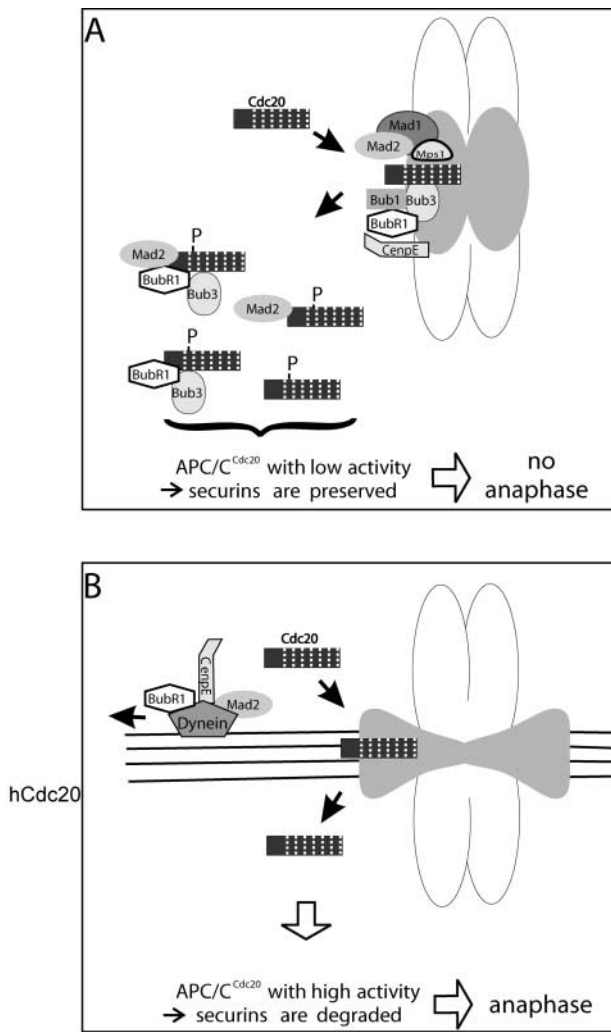
Figure 5. **Model for kinetochore-catalyzed inhibition of APC/C^{Cdc20}.** (A) The Cdc20 molecule contains an NH$_2$-terminal domain followed by a series of WD-40 repeats (stripes). Kinetochores lacking microtubule attachment and/or tension concentrate inhibitory checkpoint proteins (Mad2 and BubR1), assembly factors (Mad1 and CenpE), and checkpoint kinases (Bub1 and Mps1). Cdc20 transiently associates with kinetochores via WD-40 repeats (possibly with Bub3, another WD-40 repeat protein). While at the kinetochore, Cdc20 is modified by binding with inhibitory proteins and perhaps by other checkpoint enzymes (e.g., kinases). Various forms of Cdc20 complexed with inhibitor proteins and/or with posttranslational modifications have low activity in catalyzing APC/C-mediated transfer of ubiquitin to securins. (B) Attachment/tension of microtubules at kinetochores results in dynein-dependent depletion of spindle checkpoint proteins by transport along the spindle microtubules. After all kinetochores in the cell are attached, inhibition of Cdc20 ceases. The APC/C^{Cdc20} becomes competent to target securin for ubiquitin-mediated degradation, and anaphase initiates. During metaphase and anaphase, continued association of Cdc20 with kinetochores, centrosomes, and spindle fibers maintains active APC/C^{Cdc20} within the mitotic spindle, where its targets may be concentrated. It is not yet clear whether Cdc20 associates with kinetochores alone or in complexes with core APC/C components. For simplicity, core APC/C proteins are not depicted in the diagram, although the APC/C may also be modified (e.g., phosphorylated) by kinetochore-associated enzymes. Many other kinetochore- and spindle-associated proteins not depicted likely participate in the regulation of checkpoint signaling.

ment or tension contain high concentrations of spindle checkpoint proteins (e.g., Mad1, Mad2, Bub1, BubR1, and Bub3). We suggest that Cdc20 circulates rapidly at all kinetochores, binding via its WD-40 repeats, possibly through interaction with other WD-40 proteins, such as Bub3 (Fraschini et al., 2001). Binding to the kinetochore by the WD-40 domain leaves free the Cdc20 NH$_2$-terminal domain that contains binding sites for inhibitory checkpoint proteins Mad2 and BubR1. While at the kinetochore, Cdc20 accepts the inhibitory checkpoint proteins, and binding of anaphase inhibitors (securins) to the APC/C is blocked. In contrast, the targeting of early M phase substrates of APC/C^{Cdc20}, such as cyclin A, is not inhibited, possibly because the early substrates interact with COOH-terminal regions of Cdc20. Other kinetochore-associated checkpoint proteins (e.g., Mad1, Bub1, Mps, and CenpE) facilitate transfer of the checkpoint inhibitor proteins to Cdc20 (for Mad1 see Sironi et al., 2002). Kinetochore-bound kinases, phosphatases, or other enzymes might also modify Cdc20 or its associated proteins to inhibit APC/C^{Cdc20} targeting of securins. Microtubule attachment or tension at kinetochores induces the dynein-mediated transport of certain checkpoint proteins from the kinetochore toward the poles along spindle fiber microtubules (Howell et al., 2001). The very high exchange rates for Cdc20 (more rapid than those of the inhibitor Mad2) may allow Cdc20 to continuously sample all kinetochores within the cell and thus maintain cell-wide inhibition of APC/C^{Cdc20}, even in cells with only one or a few unattached kinetochores. Finally, during metaphase and anaphase, the continued concentration of Cdc20 at kinetochores, centrosomes, and spindle microtubules may additionally serve to maintain high levels of the active APC/C^{Cdc20} near substrates concentrated within the spindle.

Materials and methods

Cdc20–GFP constructs and mutagenesis
Oligonucleotides were synthesized for the NH$_2$- and COOH-terminal deletion mutants with an overhang sequence to allow restriction digestion after the PCR reaction. Amplified fragments were digested with HindIII and BamH1 and ligated into the pEGFP-N3 vector (CLONTECH Laboratories, Inc.) to generate fusion proteins with EGFP at the COOH-terminal end of Cdc20 mutants.

Transfection and expression of Cdc20–GFP chimeras
Cell culture was performed as previously described (Kallio et al., 1998). LLC-PK and HeLa cells were transiently transfected with plasmids encoding full-length or mutated Cdc20–GFP by LipofectAMINE PLUS reagent (Life Technologies) or Fugene 6 reagent (Roche Diagnostics Corp.) according to the manufacturer's recommendations. 24–48 h after transfection, the cells were fixed and processed for microscopic analysis or subjected to biochemical studies or live cell video analysis.

Immunoprecipitation and immunoblotting
HeLa cells expressing full-length or mutated Cdc20–GFP chimeras were treated with nocodazole or taxol for 8–12 h. Mitotic cells were collected. Cell extracts and supernatants were prepared and used for immunoprecipitation using anti-GFP antibodies (2.5 µg; Molecular Probes and Abcam Ltd.) or for Western blotting experiments as described previously (Kallio et al., 1998).

Fixation and immunofluorescence
LLC-PK cells expressing Cdc20–GFP were fixed with 3% formaldehyde in PHEM (60 mM Pipes, 25 mM Hepes, pH 6.9, 10 mM EDTA, 4 mM MgCl$_2$)

for 15 min. After washes with MBST (10 mM MOPS, 150 mM NaCl, pH 7.3, 0.05% Tween 20), DNA was stained with DAPI and the cells on coverslips were mounted with Vectashield (Vector Laboratories). For immunofluorescence, LLC-PK and HeLa cells on coverslips were simultaneously fixed and extracted for 15 min in 0.25% CHAPS in PHEM containing 2% formaldehyde and 100 nM microcystin LR. Coverslips were labeled with antibodies as previously described (Kallio et al., 1998) and analyzed with a ZEISS Axioplan IIi microscope equipped with a Hamamatsu Orca II camera and Metamorph Imaging system (Universal Imaging Corp.).

Analysis of living cells

For live cell observation, a planapochromat 60× (N.A. 1.4) objective (Nikon) was used with a SenSys CCD camera (Photometrics Ltd.) connected to a Nikon Diaphot microscope and imaged with Metamorph software. The average signal intensity of kinetochore-bound Cdc20–GFP at different mitotic phases was analyzed from 10 live cell sequences by measuring the integrated fluorescence intensity minus the background from the 10 brightest kinetochores per each cell and time point. For detailed methods on live cell analysis and FRAP see the supplemental Materials and methods (available at http://www.jcb.org/cgi/content/full/jcb.200201135/DC1).

Online supplemental material

Supplemental materials and methods, supplemental figures (Figs. S1 and S2), and Quicktime movies of the time-lapse fluorescence and phase contrast images accompanying Fig. S2 (Video 1) and Fig. 4 (Videos 2–4) are available at http://www.jcb.org/cgi/content/full/jcb.200201135/DC1.

References

Chan, G.K., S.A. Jablonski, V. Sudakin, J.C. Hittle, and T.J. Yen. 1999. Human BUBR1 is a mitotic checkpoint kinase that monitors CENP-E functions at kinetochores and binds the cyclosome/APC. *J. Cell Biol.* 146:941–954.

Chen, R.H., J.C. Waters, E.D. Salmon, and A.W. Murray. 1996. Association of spindle assembly checkpoint component XMAD2 with unattached kinetochores. *Science.* 274:242–246.

Chen, R.H., A. Shevchenko, M. Mann, and A.W. Murray. 1998. Spindle checkpoint protein Xmad1 recruits Xmad2 to unattached kinetochores. *J. Cell Biol.* 143:283–295.

Fang, G. 2002. Checkpoint protein BubR1 acts synergistically with Mad2 to inhibit the anaphase-promoting complex. *Mol. Biol. Cell.* 13:755–766.

Fang, G., H. Yu, and M.W. Kirschner. 1998. The checkpoint protein MAD2 and the mitotic regulator CDC20 form a ternary complex with the anaphase-promoting complex to control anaphase initiation. *Genes Dev.* 12:1871–1883.

Fraschini, R., A. Beretta, L. Sironi, A. Musacchio, G. Lucchini, and S. Piatti. 2001. Bub3 interaction with Mad2, Mad3 and Cdc20 is mediated by WD40 repeats and does not require intact kinetochores. *EMBO J.* 20: 6648–6659.

Gorbsky, G.J. 2001. The mitotic spindle checkpoint. *Curr. Biol.* 11:R1001–R1004.

Gorbsky, G.J., M. Kallio, J.R. Daum, and L.M. Topper. 1999. Protein dynamics at the kinetochore: cell cycle regulation of the metaphase to anaphase transition. *FASEB J.* 13:S231–S234.

Hilioti, Z., Y.S. Chung, Y. Mochizuki, C.F. Hardy, and O. Cohen-Fix. 2001. The anaphase inhibitor Pds1 binds to the APC/C-associated protein Cdc20 in a destruction box-dependent manner. *Curr. Biol.* 11:1347–1352.

Howell, B.J., D.B. Hoffman, G. Fang, A.W. Murray, and E.D. Salmon. 2000. Visualization of Mad2 dynamics at kinetochores, along spindle fibers, and at spindle poles in living cells. *J. Cell Biol.* 150:1233–1250.

Howell, B.J., B.F. McEwen, J.C. Canman, D.B. Hoffman, E.M. Farrar, C.L. Rieder, and E.D. Salmon. 2001. Cytoplasmic dynein/dynactin drives kinetochore protein transport to the spindle poles and has a role in mitotic spindle checkpoint inactivation. *J. Cell Biol.* 155:1159–1172.

Kallio, M., J. Weinstein, J.R. Daum, D.J. Burke, and G.J. Gorbsky. 1998. Mammalian p55CDC mediates association of the spindle checkpoint protein Mad2 with the cyclosome/anaphase-promoting complex, and is involved in regulating anaphase onset and late mitotic events. *J. Cell Biol.* 141:1393–1406.

Li, Y., C. Gorbea, D. Mahaffey, M. Rechsteiner, and R. Benezra. 1997. MAD2 associates with the cyclosome/anaphase-promoting complex and inhibits its activity. *Proc. Natl. Acad. Sci. USA.* 94:12431–12436.

Sironi, L., M. Mapilli, S. Knapp, A. DeAntoni, K.-T. Jeang, and A. Musacchio. 2002. Crystal structure of the Mad1-Mad2 core complex: implications of a "safety belt" binding mechanism for the spindle checkpoint. *EMBO J.* 21: 2496–2506.

Sudakin, V., G.K. Chan, and T.J. Yen. 2001. Checkpoint inhibition of the APC/C in HeLa cells is mediated by a complex of BUBR1, BUB3, CDC20, and MAD2. *J. Cell Biol.* 154:925–936.

Tang, Z., R. Bharadwaj, B. Li, and H. Yu. 2001. Mad2-independent inhibition of APCCdc20 by the mitotic checkpoint protein BubR1. *Dev. Cell.* 1:227–237.

Taylor, S.S., E. Ha, and F. McKeon. 1998. The human homologue of Bub3 is required for kinetochore localization of Bub1 and a Mad3/Bub1-related protein kinase. *J. Cell Biol.* 142:1–11.

Vodermaier, H.C. 2001. Cell cycle: waiters serving the destruction machinery. *Curr. Biol.* 11:R834–R837.

Weinstein, J. 1997. Cell cycle-regulated expression, phosphorylation, and degradation of p55Cdc. A mammalian homolog of CDC20/Fizzy/Slp1. *J. Biol. Chem.* 272:28501–28511.

Zhang, Y., and E. Lees. 2001. Identification of an overlapping binding domain on Cdc20 for Mad2 and anaphase-promoting complex; model for spindle checkpoint regulation. *Mol. Cell. Biol.* 21:5190–5199.